2010

Large dielectric tuning and microwave phase shift at low electric field in epitaxial Ba0.5Sr0.5TiO3 on SrTiO3

J. H. Leach
Virginia Commonwealth University, s2jleach@vcu.edu

H. Liu
Virginia Commonwealth University

V. Avrutin
Virginia Commonwealth University, vavrutin@vcu.edu

See next page for additional authors

Leach, J. H., Liu, H., & Avrutin, V., et al. Large dielectric tuning and microwave phase shift at low electric field in epitaxial Ba0.5Sr0.5TiO3 on SrTiO3. Journal of Applied Physics, 107, 084511 (2010).

Large dielectric tuning and microwave phase shift at low electric field in epitaxial $Ba_{0.5}Sr_{0.5}TiO_3$ on $SrTiO_3$

J. H. Leach,[1,a)] H. Liu,[1] V. Avrutin,[1] B. Xiao,[1] Ü. Özgür,[1] H. Morkoç,[1,b)] J. Das,[2,c)] Y. Y. Song,[2] and C. E. Patton[2]
[1]*Department of Electrical and Computer Engineering, Virginia Commonwealth University, Richmond, Virginia 23284, USA*
[2]*Department of Physics, Colorado State University, Fort Collins, Colorado 80523, USA*

(Received 7 January 2010; accepted 14 February 2010; published online 28 April 2010)

Dielectric properties of annealed and as-grown ferroelectric $Ba_{0.5}Sr_{0.5}TiO_3$ (BST) grown by pulsed laser deposition on sputtered BST seed layers on strontium titanate (STO) substrates were investigated at microwave frequencies in the realm of tunability of its dielectric constant as well as phase shifters based on this material. The as-grown layers were nearly fully relaxed with measured lattice parameters nearly identical to those of bulk BST. The tuning of the relative dielectric constant (~1750 at zero bias at 10 GHz) of the annealed BST was found to be as high as 59% and 56% at 10 and 19 GHz, respectively. The analysis of the loss in the BST results in a measured tan δ of 0.02 for the annealed as well as the unannealed films at a frequency of 18 GHz. Phase shifters also exhibited high tuning with differential phase shift figures of merit of 35 and 55°/dB at a field of 60 kV/cm at 10 and 19 GHz, respectively. Serendipitously, most of the tuning occurs at low fields, and thus we propose a new figure of merit, taking into account the amplitude of applied electric field in order to achieve the phase shift. In this new realm we achieved the values of this overall figure of merit of 1.2 and 1.8° cm/dB kV at 10 and 19 GHz, respectively, using an applied electric field of only 10 kV/cm. © *2010 American Institute of Physics*. [doi:10.1063/1.3359707]

I. INTRODUCTION

Ferroelectric thin film materials have steadily been gaining popularity in part due to the potential for applications in tunable microwave components. These materials generally show a high dielectric permittivity that can be controlled by application of small dc bias voltages[1,2] to give rise to potentially small, fast, and cost effective devices. $Ba_xSr_{1-x}TiO_3$ (BST),[3,4] one of the most popular ferroelectric materials, has been utilized in the demonstration of various tunable microwave components including phase shifters,[5,6] resonators,[7] and filters.[8] The high tunability of BST, desirable to achieve a large phase shift with a physically relatively small device coupled with relatively low loss at microwave frequencies, fuels the further development of this promising ferroelectric material, particularly for use in phased array antenna systems. In this manuscript, we report the high tunability of the relative permittivity of 59% at 10 GHz for films of $Ba_{0.5}Sr_{0.5}TiO_3$ grown by pulsed laser deposition (PLD) on sputtered BST seed layers on strontium titanate $SrTiO_3$ (STO) substrates and large phase shifts of 90° and 136° at 10 and 19 GHz, respectively, at an applied voltage of 30 V for a 1.5 mm long device. The high device figures of merit of 35 and 55°/dB at 10 and 19 GHz, respectively, are linked to high structural perfection of the BST layers employed.

[a)]Electronic mail: s2jleach@vcu.edu.
[b)]Electronic mail: hmorkoc@vcu.edu.
[c)]Present address: Department of Materials Science and Engineering, Virginia Tech, Blacksburg, VA 24061.

II. EXPERIMENT

BST films of thickness ~400 nm were deposited on STO substrates by off-axis radio frequency (rf) magnetron sputtering using a $Ba_{0.5}Sr_{0.5}TiO_3$ ceramic target. Details of sputtering growth conditions in general can be found in Ref. 4. This BST layer was then used as a seed layer for the subsequent growth of BST at 750 °C by PLD in a 100 mTorr oxygen atmosphere. The energy fluence and repetition rate for the 248 nm KrF laser were 1.7 J/cm^2 and 25 Hz, respectively. The deposition was done for about 1 h and the target-substrate distance was 7.5 cm. These conditions produce nominally 3 μm thick BST films on the seed layers. After growth, the sample was cut into two pieces and one piece was annealed in a tubular furnace in an O_2 ambient at 950 °C for 8 h. A trilayer lift-off procedure using a poly(methyl methacrylate) (PMMA), chromium, photoresist stack was performed to define coplanar waveguide (CPW) lines on the surface of the as-grown and annealed BST films using thick metal films of Cr/Ti/Ag/Au (50/25/2000/50 nm) deposited by electron beam evaporation. The CPW devices had a signal linewidth S of 60 μm and a separation between the edge of the signal line and the ground plane W of 5 μm. The as-grown and annealed films were characterized by high resolution x-ray diffraction (HRXRD) to assess the crystalline quality. Microwave characterization was carried out at frequencies from 1 to 20 GHz using an HP 8510B vector network analyzer.

III. ANALYSIS AND DISCUSSION

Regarding to the structural characteristics of the films, the (002) and (022) rocking curves of the as-grown and an-

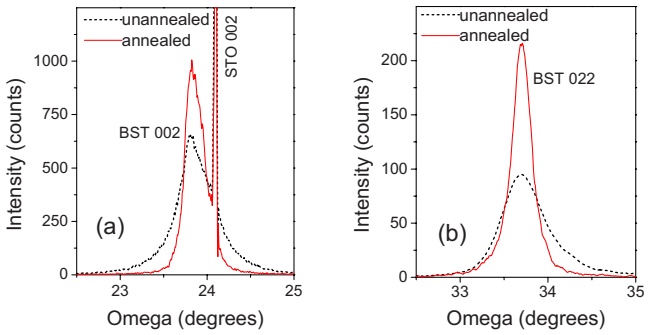

FIG. 1. (Color online) HRXRD ω rocking curve of the (a) (002) BST reflection and the (b) (022) BST reflection of as-grown (dashed lines) and annealed (solid lines) samples.

nealed BST samples are shown in Fig. 1. The BST peaks correspond to the thick PLD-grown layer. Since the lattice parameter for bulk BST (3.947 Å) is slightly higher than that for STO (3.905 Å), the sharp peak of single crystal STO appears to the right of the BST (002) rocking curve. From the XRD measurement, we determined the BST lattice parameters to be $a=3.956$ Å and $c=3.955$ Å prior to annealing and $a=3.963$ Å and $c=3.950$ Å after annealing at 950 °C. Clearly, annealing the layers results in the introduction of slight tensile strain, which may be due to the effect of the underlying (compressively strained) seed layer. As the compressively strained seed layer relaxes, the thick (initially relaxed) BST layer follows the seed layer and therefore becomes slightly tensile strained. Slightly tensile strained BST has been predicted to have a large dielectric constant, which should bode well for better device performance.[9] Furthermore, annealing appears to improve the crystalline quality of BST as the full width at half maximum (FWHM) of the symmetric (002) reflection narrows from 25.8 to 15.0 arc min and the FWHM of the asymmetric (022) reflection reduces from 33.6 to 15.0 arc min. The enhancement of the intensity of the BST reflections apparent in Fig. 1 also suggests the improved structural perfection of the annealed film, which also would bode well for better device performance. Although it is unclear whether the crystal quality or the strain plays a bigger role in the tunability of BST films, the results presented in this paper suggest that annealing can be used as a tool to introduce strain into a nearly relaxed film grown on a strained seed layer.

CPW structures served as calibration standards to perform a multiline thru-reflect-line calibration[10] using the MULTICAL software developed by National Institute of Standards and Technology (NIST). In this technique, the complex propagation constant $\gamma=\alpha+j\beta$ is determined as a function of frequency from which the effective relative permittivity is determined through the following equation:[11]

$$\varepsilon_{r,\mathrm{eff}} = -\left(\frac{c\gamma}{\omega}\right)^2. \tag{1}$$

Using this effective relative permittivity value, we can determine the dielectric constant of the BST layer itself, ε_{r2}, using the closed form expression found from conformal mapping as follows:[12]

$$\varepsilon_{r,\mathrm{eff}} = 1 + (\varepsilon_{r1} - 1)\left[\frac{1}{2}\frac{K(k_1)}{K(k_1')}\frac{K(k_0')}{K(k_0)}\right] + (\varepsilon_{r2} - \varepsilon_{r1}) \times \left[\frac{1}{2}\frac{K(k_2)}{K(k_2')}\frac{K(k_0')}{K(k_0)}\right], \tag{2}$$

where ε_{r1} and ε_{r2} are the dielectric constants of the substrate and BST layer, respectively, $K(k)$ is the complete elliptic integral of the first kind, $k_0=k_1=S/(S+2W)$ with S being equal to the signal linewidth and W to the separation between the edge of the signal line and ground plane, $k_2=\sinh(\pi S/4h_2)/\sinh[\pi(S+2W)/4h_1]$ with h_1 and h_2 being equal to the thicknesses of the STO substrate and the BST film, respectively, and $k_i'=\sqrt{1-k_i^2}$. The terms in square brackets can be referred to as q_1 and q_2, the filling factors of the substrate and BST films, respectively. The thickness of the BST films was determined by cross-sectional scanning electron microscopy to be about 3 μm. This value is critical for accurately determining the dielectric constant of the film.

We have used a relative dielectric constant of 300 for the STO substrate as determined by a separate calibration on a bare STO substrate. Figure 2(a) shows the effective dielectric constant for both the as-grown (open symbols) and the annealed (closed symbols) BST films versus applied electric field. Note that we use a simple estimation (uniform field) of the electric field by dividing the bias voltage by W. Of course, this is an overestimation of the actual field within the BST layer since the contacts reside on the surface of the sample and therefore the field would decrease with depth in

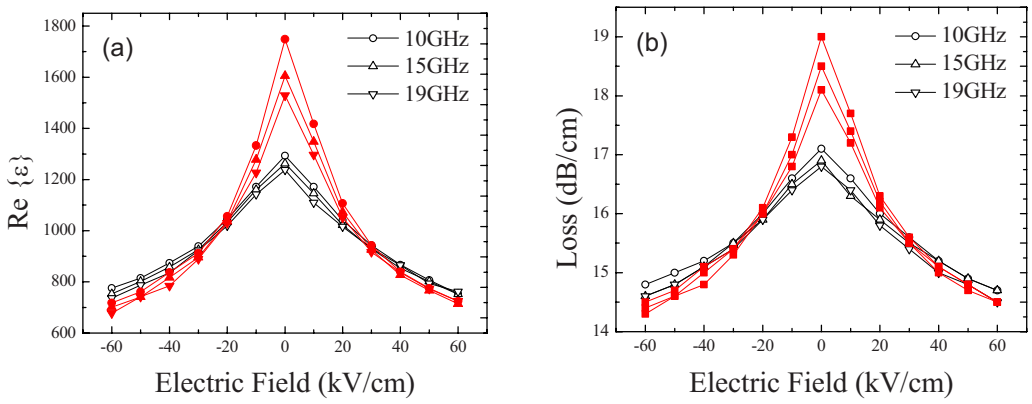

FIG. 2. (Color online) (a) Measured relative dielectric constant and (b) loss of the BST layers grown on STO on sputtered seed layers before (open symbols) and after (closed symbols) annealing at 950 °C for 8 h.

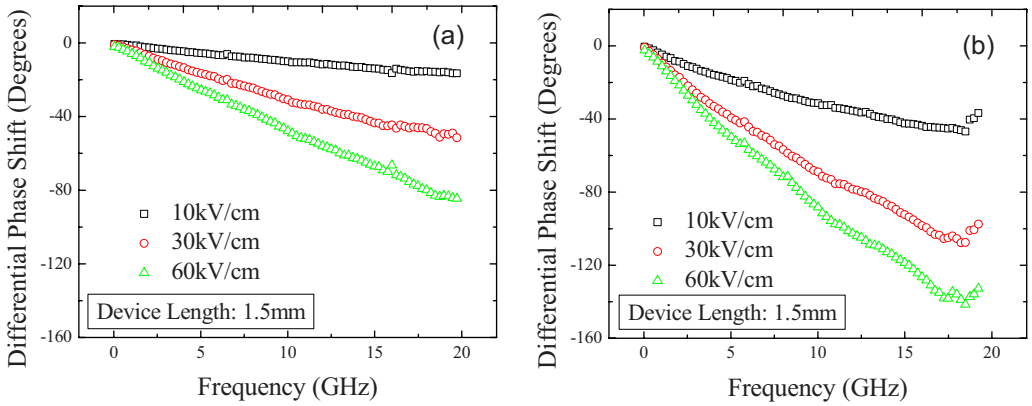

FIG. 3. (Color online) Measured differential phase shift for a 1.5 mm device under various applied fields for (a) as-grown and (b) annealed BST layers.

the film. The tuning of the dielectric constant at 60 kV/cm (corresponding to an applied bias of 30 V if uniform field is assumed) for the as-grown sample is 42% and 40% at 10 and 19 GHz, respectively, while the tuning for the annealed film increases to 59% and 56% at 10 and 19 GHz, respectively. This improvement in the value of dielectric constant and its tuning is consistent with the improvement in crystalline quality as well as the slight tensile strain introduced after annealing, as indicated by the HRXRD data shown in Fig. 1.

Figure 2(b) displays the loss (α) in units of dB/cm of the CPW lines determined directly from the calibration procedure described above. As expected, the loss decreases with increasing bias electric field. A part of the reason for the relatively large loss of the lines is the inherent conductor loss associated with the geometry of the particular CPW structures employed. As discussed in Ref. 13, the optimal characteristic impedance Z_0 of a CPW line is around 50 Ω. In order to achieve such a Z_0 value on a substrate with a large dielectric constant (i.e., the BST with a dielectric constant over 1000), an unreasonably narrow center line or a ground plane separation, which is larger than that which could be supported by the pitch of the on wafer probes employed (150 μm), would be necessary. It would also increase the bias voltage required to reach the same electric field. In fact, an identical calibration using the same CPW geometry on a bare STO substrate (with measured relative dielectric constant of ~300) results in a loss of 12 ± 0.2 dB/cm at frequencies between 10 and 20 GHz.

It is useful to attempt to estimate the actual loss of the BST films (i.e., tan δ) so that we can determine their inherent properties. In order to perform such an estimate, we can again use expressions derived from the conformal mapping analysis. We will assume that all of the loss in the system is due to either the conductor loss α_c or dielectric loss α_d (i.e., no radiation or surface wave losses). Under the aforementioned assumption, the total loss is simply the sum of the conductor and dielectric losses,

$$\alpha = \alpha_c + \alpha_d. \tag{3}$$

We first estimate the conductor loss as[12]

$$\alpha_c = \frac{R_{\text{center}} + R_{\text{ground}}}{2Z_0}, \tag{4}$$

where R_{center} and R_{ground} represent the series resistances per unit length of the center and ground conductor planes, respectively,[12]

$$R_{\text{center}} = \frac{R_{\text{skin}}}{4S(1-k_0^2)K^2(k_0)}\left\{\pi + \ln\left(\frac{4\pi S}{t}\right) - k_0\left(\frac{1+k_0}{1-k_0}\right)\right\}, \tag{5}$$

$$R_{\text{ground}} = \frac{k_0 R_{\text{skin}}}{4S(1-k_0^2)K^2(k_0)}\left\{\pi + \ln\left(\frac{4\pi(S+2W)}{t}\right) - \frac{1}{k_0}\left(\frac{1+k_0}{1-k_0}\right)\right\}, \tag{6}$$

where t is the metal thickness, assumed to be much thicker than the skin depth, and

$$R_{\text{skin}} = \frac{1}{\delta\sigma} \tag{7}$$

is the surface resistance due to the skin effect. Here δ is the skin depth and σ is the conductivity of the metal. We use a 2 μm thick metal and a conductivity of 6.173×10^7 S/m for the calculations (representing the thickness and conductivity of the silver in the metal stack).

Utilizing the above mentioned numbers we can obtain the metal contribution to the loss at high frequencies, i.e., where the metal thickness is $>4\delta$. At 18 GHz, we obtain a metal-related loss of 8.0, 11.2, and 12.1 dB/cm for metal films on a bare STO wafer and on the unannealed and annealed layers of BST on STO, respectively. Clearly, the metal contribution to the loss is dominant due to the nonoptimal geometry of the device and subsequent low characteristic impedances. We can obtain tan δ associated with the dielectric by extracting the loss component associated with the metal from the overall measured loss using Eq. (3) and the expression for the dielectric loss,[12]

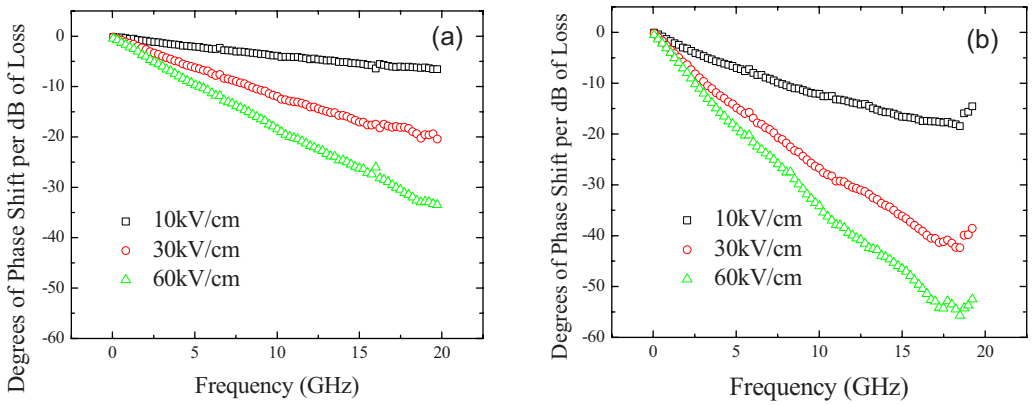

FIG. 4. (Color online) Measured figure of merit (differential phase shift in degrees per loss in decibel) for various applied fields for (a) as-grown and (b) annealed BST layers.

$$\alpha_d = \frac{\pi}{\lambda_0}\frac{\varepsilon_r}{\sqrt{\varepsilon_{\text{eff}}}} q \tan \delta. \tag{8}$$

For the bare STO substrate, we deduce tan δ to be 0.0098 at 18 GHz. For the BST on STO layers, we can write the following expression to deduce the effective tan δ of the BST/STO system after Eq. (8):

$$\alpha_d = \frac{\pi}{\lambda_0}\frac{1}{\sqrt{\varepsilon_{\text{eff}}}}\{\varepsilon_{r1}q_1 + \varepsilon_{r2}q_2\}\tan \delta_{\text{eff}}. \tag{9}$$

From this, we obtain the effective tan δ, tan δ_{eff} of the unannealed and annealed films to be 0.018 at 18 GHz. Finally, in order to obtain the loss tangent of the BST film alone, we write

$$\varepsilon_{\text{eff}} \tan \delta_{\text{eff}} = q_1\varepsilon_{r1} \tan \delta_1 + q_2\varepsilon_{r2} \tan \delta_2 \tag{10}$$

and obtain the loss tangents of the BST films to be 0.02 at 18 GHz for both the unannealed and annealed films. It is interesting to note that despite the improvement in crystal quality, the dielectric loss is unchanged after annealing. With these results, an intrinsic figure of merit, which is defined as the tunability (in percent) divided by tan δ, would be ~2000 and ~2500 for the unannealed and annealed layers, respectively, near 20 GHz at an applied voltage of 30 V.

Next, the differential phase shift along the CPW lines was measured as a function of applied field. These results are displayed in Fig. 3 for CPW lines with a length of 1.5 mm fabricated on both the as-grown and annealed samples. At a bias voltage of 30 V, we observed a differential phase shift of 48° and 82° at 10 and 19 GHz, respectively, for the as-grown layer and a differential phase shift of 90° and 136° at 10 and 19 GHz, respectively, for the annealed sample.

Using the measured loss at zero field (where the loss is at its maximum) as a function of frequency and normalizing the differential phase shift to unit length, we can determine the typically reported figure of merit for these devices in terms of degrees of phase shift per decibel of loss (Fig. 4). We obtain a figure of merit of 19 and 33°/dB at 10 and 19 GHz, respectively, for the as-grown layer and a figure of merit of 35 and 55°/dB at 10 and 19 GHz, respectively, for the annealed sample. It is remarkable that these figures of merit, particularly those for the device fabricated on the annealed layer, compare well with some of the best ones reported in the literature considering the relatively large amount of loss present in the devices.[5,6,14,15] Further work involving more sophisticated phase shifter designs, such as those presented in Refs. 5 and 14, can vastly improve the performance in terms of loss.

Finally, we wish to comment on the use of an alternative figure of merit, taking into account the strength of electric field required to achieve a given phase shift. As the voltage required to realize a given phase shift is important in actual devices in real systems, we propose to simply divide the traditional figure of merit by the applied field, which yields a figure in units of ° cm/dB kV, and allows one to more effectively compare devices produced in different laboratories. Table I displays this new figure of merit for our devices as well as for devices from other laboratories for comparison. For all the devices, we define the field to be simply the voltage divided by the separation between the electrodes that generate the tuning (in our case, between the signal and

TABLE I. Comparison of experimentally achieved figure of merit for various types of phase shifters for various laboratories.

Figure of merit (deg cm/dB kV)	Bias voltage (V)	Frequency (GHz)	Type of phase shifter	Ref.
0.40	20	23.7	Coupled microstrip	6
0.22	5	10	Parallel plate loaded CPW	5
0.18	10	20	IDC loaded CPW	14
1.14	20	20	CPW	15
1.8	5	19	CPW	This work

ground planes which is 5μ). As mentioned above, this overestimates the actual field in the BST layer for coplanar structures. Therefore, our estimation of the improved figure of merit is a conservative one. For our CPW structures, we achieve 1.2 and 1.8° cm/dB kV at 10 and 19 GHz, respectively, for the annealed sample. Note that this value does not correspond to the maximum applied field for our layers. It is interesting that the highest values for this alternative figure of merit are achieved using simple CPW designs (this work and Ref. 15), which do not involve any periodic loading of a synthetic transmission line.

IV. CONCLUSIONS

We have demonstrated very high tuning and relatively low loss on BST layers deposited by PLD on sputtered BST seed layers at microwave frequencies. Annealing of the BST films resulted in an improvement of crystalline quality and subsequently an increase in tunability. A phase shift of 55°/dB at 19 GHz was achieved, which translates to an overall alternative figure of merit of 1.8° cm/dB kV if the applied electric field was taken into account, as described in the text. We expect this alternative figure of merit to be useful in comparing devices from different laboratories, taking into consideration the geometry as well as the general phase shifter designs. At present, the design of the phase shifter limits the usefulness as the loss is dominated by metal losses as opposed to the losses associated with the BST layer. At this stage it is not sufficiently clear whether the improvement of the crystal quality or the slight tensile strain that is introduced after annealing is the driving force behind the improvement in tunability. If the introduction of strain is in fact the key, one could envision using strained seed layers prior to the growth of bulklike BST by PLD and gain the ability to effectively tune the amount of strain delivered to the PLD layer through a careful selection of annealing conditions.

ACKNOWLEDGMENTS

The authors would like to thank Dr. W. Chang, Dr. L. M. B. Alldredge, Dr. S. W. Kirchoefer, and Dr. J. M. Pond at the Naval Research Laboratory for fruitful discussions. This work is funded by the Office of Naval Research under the directions of Dr. I. Mack and Dr. D. Green.

[1] A. K. Tagantsev, V. O. Sherman, K. F. Astafiev, J. Venkatesh, and N. Setter, J. Electroceram. **11**, 5 (2003).
[2] N. Izyumskaya, Ya. I. Alivov, and H. Morkoç, Crit. Rev. Solid State Mater. Sci. **34**, 89 (2009).
[3] L. M. B. Alldredge, W. Chang, S. B. Qadri, S. W. Kirchoefer, and J. M. Pond, Appl. Phys. Lett. **90**, 212901 (2007).
[4] B. Xiao, V. Avrutin, H. Liu, E. Rowe, J. Leach, X. Gu, Ü. Özgür, H. Morkoç, W. Chang, L. M. B. Alldredge, S. W. Kirchoefer, and J. M. Pond, Appl. Phys. Lett. **95**, 012907 (2009).
[5] B. Acikel, T. R. Taylor, P. J. Hansen, J. S. Speck, and R. A. York, IEEE Microw. Wirel. Compon. Lett. **12**, 237 (2002).
[6] C. L. Chen, J. Shen, S. Y. Chen, G. P. Luo, C. W. Chu, F. A. Miranda, F. W. Van Keuls, J. C. Jiang, E. I. Meletis, and H. Y. Chang, Appl. Phys. Lett. **78**, 652 (2001).
[7] A. B. Ustinov, V. S. Tiberkevich, G. Srinivasan, A. N. Slavin, A. A. Semenov, S. F. Karmanenko, B. A. Kalinikos, J. V. Mantese, and R. Ramer, J. Appl. Phys. **100**, 093905 (2006).
[8] A. Tombak, J. P. Maria, F. T. Ayguavives, Z. Jin, G. T. Stauf, A. I. Kingon, and A. Mortazawi, IEEE Trans. Microwave Theory Tech. **51**, 462 (2003).
[9] N. A. Pertsev, A. G. Zembilgotov, and A. K. Tagantsev, Phys. Rev. Lett. **80**, 1988 (1998).
[10] R. B. Marks, IEEE Trans. Microwave Theory Tech. **39**, 1205 (1991).
[11] D. C. DeGroot, J. A. Jargon, and R. B. Marks, 60th Automatic RF Techniques Group (ARFTG) Conference Digest, 2002 (unpublished), pp. 131–155.
[12] R. N. Simons, *Coplanar Waveguide Circuits, Components, and Systems* (Wiley-Interscience, New York, 2001).
[13] T. Kitazawa and T. Itoh, IEEE Trans. Microwave Theory Tech. **39**, 1694 (1991).
[14] G. Vélu, K. Blary, L. Burgnies, J.-C. Carru, E. Delos, A. Marteau, and D. Lippens, IEEE Microw. Wirel. Compon. Lett. **16**, 87 (2006).
[15] H.-S. Kim, I.-D. Kim, K.-B. Kim, T.-S. Yun, J.-C. Lee, H. L. Tuller, W.-Y. Choi, and H.-G. Kim, J. Electroceram. **17**, 421 (2006).